Block Copolymer Mixtures As Revealed by Neutron Reflectivity

A. M. Mayes

Department of Materials Science and Engineering, Massachusetts Institute of Technology, Cambridge, Massachusetts 02139

T. P. Russell* and V. R. Deline

IBM Research Division, Almaden Research Center, 650 Harry Road, San Jose, California 95120-6099

S. K. Satija and C. F. Majkrzak

Reactor and Radiation Division, National Institute of Standards and Technology, Gaithersburg, Maryland 20899

Received April 25, 1994; Revised Manuscript Received September 7, 1994[⊗]

ABSTRACT: Thin film mixtures of high and low molecular weight symmetric poly(styrene-*b*-methyl methacrylate) diblock copolymers were investigated by neutron reflectivity. The preferential interaction of the block components with the surface and substrate causes the mixtures to organize upon annealing into alternating lamellar microdomains of PS and PMMA oriented parallel to the substrate surface. By deuterating the PMMA blocks of both mixture components, the periodicity and interfacial width were determined as a function of the mixture composition. The lamellar period, d, of the mixture was found to scale approximately with the number-average molecular weight as $d \sim M_n^{2/3}$. Via selective deuteration, the copolymer block distributions within the domains were obtained by combining results from complementary experiments. In all cases investigated, nonuniform profiles were observed whereby the shorter copolymer chains localized to the PS/PMMA interface regions while longer chains enriched the domain centers.

1. Introduction

The self-assembling nature of block copolymers is central to their commercial role as surfactants, adhesives, and thermoplastic elastomers.[1] Beyond traditional applications, the synthesis of novel block copolymer systems has established these materials as promising candidates for future device technologies. Copolymers with charge-conducting blocks[2,3] could eventually find use in flexible circuits and conductive coatings. Aggregated copolymer chains could function as nanoscale reactors, where reactants and products are confined to ordered domains of one block type.[4] A recently discovered copolymer system which exhibits a miscibility window between high- and low-temperature ordered phases could have applications in thermal sensors or switches.[5]

As the end-use technology for copolymer systems shrinks to the scale of the molecules themselves, the ability to control and manipulate their ordered-state morphology becomes increasingly important. It is well-established both theoretically[6–9] and experimentally[10–12] that the periodicity of an ordered copolymer melt is determined primarily by the copolymer molecular weight, whereas the structure itself (i.e., lamellae, cylinders, spheres) is a strong function of the relative block fractions. In strongly segregated systems, the periodicity d of a narrow molecular weight distribution copolymer in the melt is known to scale with the degree of polymerization, N, as $d \sim N^{2/3}$. While precise control over molecular weight (or N) is impractical on commercial scales, other means can be devised to variably tune the final copolymer period and/or structure. For instance, a homopolymer compatible with one block might be added to a copolymer in order to vary the relative fractions of the block microdomains and thereby control the structure.[13–16] Similarly, a second block copolymer of roughly equal composition but different molecular weight can be added to tune the period while preserving the structure and composition.[17–19] This paper examines thin film mixtures of high and low molecular weight block copolymers of poly(styrene-*b*-methyl methacrylate), P(S-*b*-MMA). Neutron reflectivity is employed to study the influence of mixture composition on copolymer periodicity and to characterize segmental profiles within ordered copolymer microdomains.

A number of notable studies have been reported on binary block copolymer mixtures in the bulk.[17–20] Hadzioannou and Skoulios[17] performed small-angle X-ray and neutron scattering (SAXS and SANS) studies on mixtures of compositionally symmetric or nearly symmetric copolymers of poly(styrene-*b*-isoprene), P(S-*b*-I). Binary mixtures of diblocks and mixtures of diblocks and triblocks exhibited complete miscibility, with lamellar repeat periods intermediate between the equilibrium values of the pure components. For a number of the mixtures, a linear variation in the period was observed as a function of mixture composition. Other systems showed positive deviations from ideal mixing. Hashimoto[18] reexamined the data from this study and found that, for several of these latter systems, the variation in d with the number-average molecular weight of the mixture was well described by the scaling relation $d \sim M_n^{2/3}$, where

$$M_n = \sum x_i M_{n,i} \tag{1}$$

and x_i is the mole fraction of mixture component i having a number-average molecular weight $M_{n,i}$.

More recently, Hashimoto and co-workers analyzed binary mixtures of symmetric P(S-*b*-I) diblocks over a wider range of component molecular weights using SAXS and transmission electron microscopy (TEM).[19,20]

[⊗] Abstract published in *Advance ACS Abstracts,* November 1, 1994.

0024-9297/94/2227-7447$04.50/0

When the molecular weight ratio between mixture components was larger than ~5, mixtures were found to separate macroscopically into two ordered phases of distinct periodicities for some range in mixture composition. For fully miscible systems, the domain spacing obeyed the scaling relation $d \sim M_n^{2/3}$. While the results from these studies clearly indicate that mixing occurs at the molecular scale, the segment distribution of long and short copolymer components within the ordered domains cannot be readily addressed using these characterization methods.

Bates and co-workers[21] studied binary mixtures of poly(ethylenepropylene-*b*-ethylethylene) diblocks by dynamic mechanical analysis. Their work focused on the weak segregation limit of the phase diagram,[22] i.e., mixtures near the disorder–order transition, to determine the influence of mixture composition on the transition. Their results suggest the existence of a biphasic region over a defined temperature range for a given mixture composition. In this region, an ordered phase rich in the high molecular weight component would exist in equilibrium with a disordered phase rich in the low molecular weight component, with the relative fractions of each phase dictated by the lever rule.

In the present study, neutron reflectivity is used to reveal details of the morphology of ordered copolymer mixtures, inaccessible by bulk characterization techniques. Thin film mixtures of high and low molecular weight symmetric poly(styrene-*b*-methyl methacrylate) diblock copolymers are analyzed as models for bulk mixtures. Due to preferential surface–block interactions, such films organize into alternating lamellar microdomains of PS and PMMA oriented parallel to the silicon surface.[23–26] By deuterating the PMMA blocks of both mixture components, the domain periodicity and interfacial width are determined to within a few angstroms for different mixture compositions. More significantly, the spatial distributions of the high and low molecular weight copolymer blocks are determined from reflectivity experiments on mixtures containing one component with one isotopically labeled block. In all cases studied, it is shown that the distribution of high and low molecular weight components is nonuniform within the lamellar microdomains, with short chains preferentially located at the interface between the PS and PMMA layers. Such detailed knowledge of copolymer organization is important as we seek to control the functionality of copolymer systems on the molecular scale.

2. Experimental Section

Anionically synthesized poly(styrene-*b*-methyl methacrylate) diblock copolymers were purchased from Polymer Laboratories. All copolymers were roughly symmetric in block composition so that, in the ordered state, their equilibrium morphology is lamellar. Molecular weight, labeling, and composition characteristics of the copolymers used in this work are given in Table 1. Prior to use, any polystyrene homopolymer impurities generated in the copolymer syntheses were removed by refluxing cyclohexane over the copolymers in a Soxhlet extraction unit overnight. Solutions were prepared as 2–3% w/v copolymer in toluene, a good solvent for PS and PMMA.

Thin films (1000–2000 Å) of the copolymer mixtures were obtained by spin coating onto polished silicon substrates 10 cm in diameter. Prior to use, the substrates were immersed in a Chromerge/chromic acid solution overnight and rinsed in deionized water. Substrates were next placed in a Nochromix/sulfuric acid bath for 5 min, rinsed thoroughly with deionized water, and exposed to isopropyl alcohol vapor for several minutes. This cleaning procedure leaves a passivating oxide layer ~15 Å thick on the surface of the silicon.

Table 1. Characteristics of the Diblock Copolymers

copolym	abbrevn	$M_{w,C}$[a]	M_w/M_n[b]	f_{PS}[c]
P(S-*b*-MMA)	30K	33 900	1.08	0.54
P(S-*b*-d-MMA)	30K	29 800	1.09	0.48
P(d-S-*b*-MMA)	30K	27 700	1.08	0.45
P(S-*b*-MMA)	110K	114 000	1.09	0.51
P(S-*b*-d-MMA)	120K	121 000	1.12	0.45
P(d-S-*b*-MMA)	100K	101 000	1.07	0.52
P(S-*b*-MMA)	300K	283 000	1.08	0.53
P(S-*b*-d-MMA)	300K	289 000	1.07	0.47
P(d-S-*b*-MMA)	300K	310 000	1.08	0.57

[a] $M_{w,C}$ is the weight-average molecular weight of the copolymer. [b] M_w/M_n is the polydispersity of the copolymer. [c] f_{PS} is the volume fraction of PS in the copolymer.

Mixtures were prepared by codissolving a $\sim 1 \times 10^5$ molecular weight (100K) copolymer material with varying fractions of either a $\sim 3 \times 10^5$ molecular weight (300K) copolymer or a $\sim 3 \times 10^4$ molecular weight (30K) copolymer (see Table 1). The 30K materials used in this study are disordered systems in the bulk at the annealing temperature. Films of the copolymer mixtures were annealed at 170 °C for several days under vacuum to induce orientation of the lamellar domains parallel to the substrate. Ellipsometry was performed prior to annealing to obtain a measure of the initial film thicknesses. After annealing, samples were examined by optical microscopy for signs that orientation was complete, namely, the appearance of integral steps on the film surface and/or sharply defined interference fringes at the film edges.[23]

Neutron reflectivity measurements were performed on the BT-7 instrument at the National Institute of Standards and Technology. The experimental setup and sample alignment procedure have been described previously.[16,25] A graphite monochromator is used to deliver neutrons of wavelength 2.37 Å to the sample, with a wavelength resolution $\Delta\lambda/\lambda \approx 0.01$. The reflectivity curves are generated by rotating the sample Θ and the detector 2Θ with respect to the incident beam. Background intensity was measured by offsetting 2Θ by $+0.25°$. After subtracting background intensity, the reflectivity is normalized by dividing the reflected intensity by the main beam intensity for the same slit configuration.

The reflectivity data was modeled following procedures outlined in earlier publications.[16,27,28] Model scattering length density (b/V) profiles were generated by dividing the ordered copolymer films into numerous layers and calculating the b/V value for each layer from an assumed form for the concentration profile within the copolymer domains. The theoretical reflectivity was then derived from the model b/V profile and compared to the experimental data. Model parameters were modified iteratively to achieve a best fit to the data.

To determine the variation in copolymer period as a function of mixture composition, systems were prepared in which the PMMA blocks of both mixture components were fully deuterated. Fits to the reflectivity profiles obtained for these systems provide both the average period and interfacial width. To study the spatial distribution of high and low molecular weight copolymer blocks within the layers, equivalent mixtures were prepared in which one component had one deuterated block. To characterize completely the block distribution profile of a given mixture composition, three equivalent systems were investigated. For mixtures composed of three effective components (one deuterated and two hydrogenated monomer species) it was necessary to deconvolute the b/V profiles into volume fraction profiles. This was facilitated using the average values of the interfacial width obtained from the strong scattering systems. Knowing the volume fractions of the three species, the b/V values for each model layer can be converted into the three weighted contributions.

3. Results and Discussion

Figures 1 and 2 show reflectivity data from two series of binary diblock mixtures in which the PMMA blocks

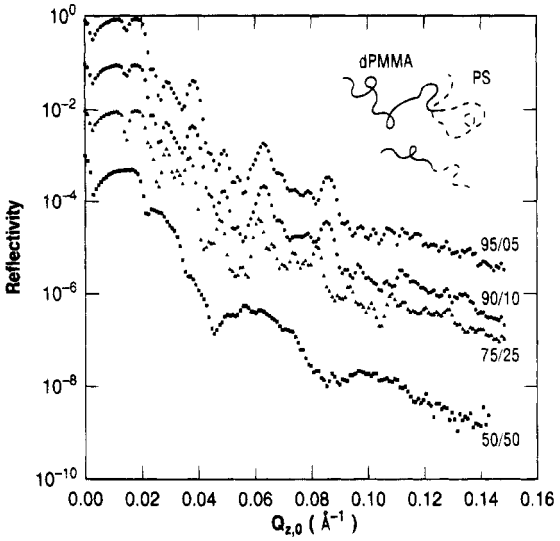

Figure 1. Reflectivity data for 120K/300K block copolymer mixtures of weight composition 95:05 (a), 90:10 (b), 75:25 (c), and 50:50 (d).

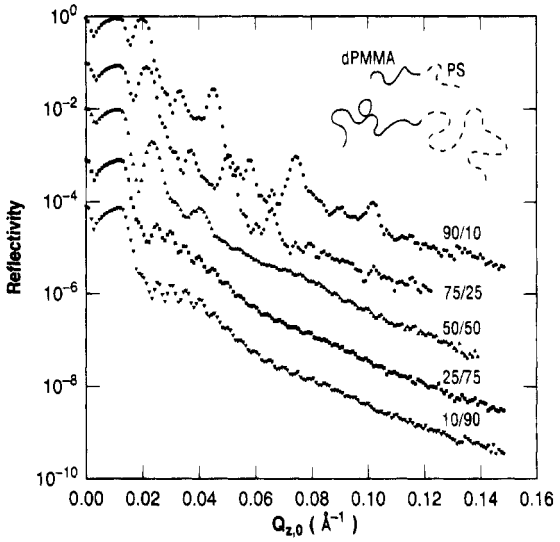

Figure 2. Reflectivity data for 120K/30K mixtures of weight composition 90:10 (a), 75:25 (b), 50:50 (c), 25:75 (d), and 10:90 (e).

of both copolymers are labeled with deuterium. Results from 120K/300K mixture compositions of 95:05, 90:10, 75:25, and 50:50 are shown in Figure 1a–d, respectively. The reflectivity profiles have been offset vertically for clarity. The strong Bragg reflections evident in parts a–c show that these films are highly ordered, with the lamellar microdomains oriented parallel to the substrate. A shift in the reflections to lower k values ($k = 2\pi/\lambda \sin \Theta$) with increasing concentration of the 300K copolymer indicates an increase in the period resulting from the incorporation of the longer copolymer chains. In the 50:50 mixture, however, the Bragg reflections disappear. This profile could not be fit satisfactorily using a uniform multilayer model. One possible explanation for this is that phase separation of the two copolymers has occurred, similar to that observed by Hashimoto and co-workers[19,20] in bulk copolymer mixtures. The component molecular weight ratio, 2.5, is well below the limit of ~5 suggested as a criterion for complete miscibility. The miscibility limit might be expected to shift to smaller ratios, however, with increasing number-average molecular weight of the mixture, since the entropic penalty for demixing becomes smaller.

Interference microscopy measurements on the 50:50 mixture indicated that a well-ordered multilayered structure had formed, as evidenced by the discrete changes in the interference colors at the edge of the sample and the formation of islands on the surface of the film. The interference color of the islands was uniform and only one color was observed which limits the extent of a lateral phase separation of the copolymers to the micron size scale or less. If a coarse phase separation did occur laterally, either two different step heights of the islands would have been observed or the background color would have been nonuniform. Alternatively, a phase separation normal to the surface was considered. Optical microscopy would not be sensitive to such a phase separation. From the reflectivity results it is evident that the critical angle of the 50:50 mixture is much higher than the critical angles of the other 120K:300K mixtures. Since the critical angle depends upon the average scattering length density of the films, which does not change with composition, then such an increase in the critical angle was not expected. However, if there are several periods in the multilayered structure, then combined first-order reflections could give rise to the observed increase in the critical angle. Such an increased effective critical angle, in fact, forms the basis of supermirrors used to guide neutrons over large distances.[29,30] While such a phase separation normal to the film surface is speculative, it does provide a reasonable description of the optical microscopy and reflectivity results.

The addition of a lower molecular weight (30K) copolymer to the 120K material correspondingly results in a decrease of the lamellar period. Figure 2 shows the reflectivity profiles from 120K/30K mixtures having compositions of 90:10, 75:25, 50:50, 25:75, and 10:90 in curves a–e, respectively. As the fraction of 30K material increases, the Bragg reflections shift to higher k values and finally disappear. Only a shoulder in the reflectivity profile remains for systems with more than 75 wt % of the 30K component. This shoulder is a signature of composition modulations propagating from the air and/or substrate interfaces, as observed previously in studies on thin films of disordered block copolymers.[28,31] The absence of a first-order Bragg reflection at low k values suggests that the biphasic morphology discussed by Bates and co-workers[21] is not formed within these film mixtures.

Reflectivity profiles from the ordered mixture systems are readily fit using scattering length density profiles assuming alternating layers of PS and labeled PMMA, with concentration gradients between the microdomains having a hyperbolic tangent form. Such models have been used successfully to describe film morphologies of ordered copolymers[25] and copolymer/homopolymer blends,[27] yielding the domain sizes and average interfacial width to an accuracy of several angstroms. Figure 3 presents a log–log plot of the domain spacing as a function of M_n, calculated from eq 1, for the two sets of mixtures. Numerical values for the domain spacing are given in Table 2. The linear best fit to the data yields a slope of 0.63. The line drawn in the figure has a slope of $^2/_3$ which corresponds to the power law suggested by Hashimoto et al.[19] from their studies on bulk mixtures and from neat diblock copolymers in the strong segregation limit.[10–12] It is interesting to note that the $^2/_3$ power law extends from the pure 29.8K copolymer to the 289K copolymer. This result is somewhat unexpected since, in the bulk, the 289K copolymer is in the strong

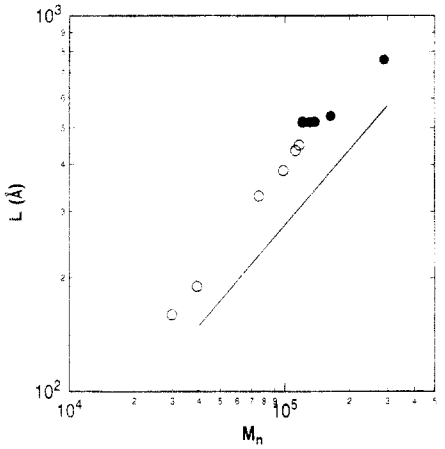

Figure 3. Scaling of the domain spacing as a function of number-average molecular weight from data collected on ordered 120K/30K (○) and 120K/300K (●) mixtures. The linear best fit to the data yields a slope of 0.63.

Table 2. Molecular Weight Dependence of the Copolymer Period

$M_n \times 10^{-3}$ [a]	L (Å)	$M_n \times 10^{-3}$ [a]	L (Å)
29.8[b]	160	121.3[b]	518
39.0	190	129.7	518
75.5	330	138.1	519
98.4	38.5	163.3	538
112.1	435	289.2[b,c]	760
116.7	450		

[a] Calculated according to eq 1. [b] Data for pure copolymer. [c] Obtained from ref 25.

segregation limit whereas the 28.9K copolymer is in the weak segregation regime. The $^2/_3$ power law suggests that all the systems are in the strong segregation regime however. This may be a ramification of the finite size of the sample. It has been established that the proximity of the air/polymer and polymer/substrate interfaces causes the order–disorder transition or the upper critical ordering transition temperature, T_{UCOT}, to shift to higher temperatures with decreasing film thickness. Thus, for a given temperature, this shift in the transition temperature will place all the copolymers in a more strongly segregated regime.

The average interfacial width for the 120K/300K mixtures with oriented lamellae parallel to the surface exhibited no variation as a function of the composition. In all cases the measured interfacial width was 50 ± 3 Å. This result is not greatly surprising since reflectivity measurements on pure P(S-*b*-MMA) diblocks of comparable molecular weights have also yielded this value.[25] Self-consistent-field calculations predict an interfacial width about 10 Å smaller than that observed. The discrepancy can be explained on the basis of interface fluctuations, as discussed recently.[32] The effective interfacial width measured experimentally is a convolution of the intrinsic width and waviness of the interface.

As 30K copolymer is added to the 120K material, the interfacial width is seen to broaden. With 10 wt % of the short chains incorporated in the lamellar structure, the interfacial width increases to ~55 Å. At 25 wt % it reaches 70 Å, though the system remains fully ordered. To explain how the incorporation of a low molecular weight copolymer effects a broadening of the interfacial width, the distributions of the two copolymer components within the ordered domains must be characterized.

The reflectivity profile for a 90:10 mixture of an unlabeled 110K diblock copolymer with a 30K P(d-S-*b*-MMA) is shown in Figure 4. The solid line in the figure is the best fit to the reflectivity profile calculated using the scattering length density profile in the inset. The shallow maxima in the *b*/*V* profiles indicate that there is an excess of deuterated PS at the microdomain interfaces, implying a localization of the low molecular weight material to the interfacial region. In the fitting procedure, the parameters are varied independently for each domain of the film. The fact that the *b*/*V* profile is consistent from domain to domain in Figure 4 is evidence that the film is well equilibrated and that the mixing is uniform. Using the value for the interfacial width determined from the 90:10 results in Figure 2, the *b*/*V* profile can be deconvolved into volume fractions of PS, d-PS, and PMMA. The volume fraction profiles for one characteristic domain of this mixture are shown in Figure 5. The distribution of labeled polystyrene (●) peaks within the interface between the PS (○) and PMMA (◇) domains. The d-PS blocks are distributed asymmetrically, with some portion extending into the PS domains. The blocks do not appear to reach the domain center, however. The integrated volume fraction of d-PS in the PS domains is ~7.0%, which is notably lower than the calculated value of 9.3%.

A similar picture emerges in the analysis of the reflectivity data from an analogous 90:10 mixture of the unlabeled 110K with a 30K P(S-*b*-d-MMA). The reflectivity profile for this mixture, along with the calculated reflectivity profile, and the corresponding scattering

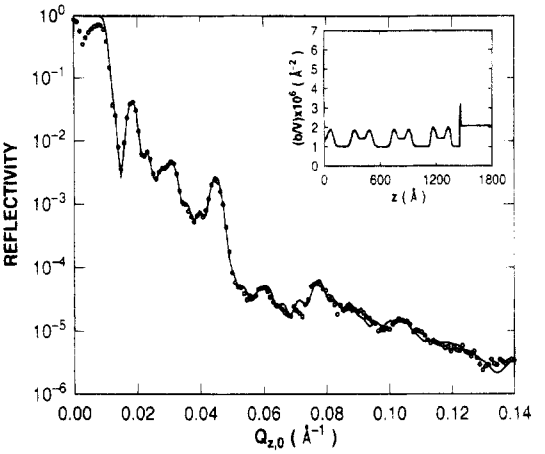

Figure 4. Fitted reflectivity data and model scattering length density profile (inset) for a 110K/30K mixture of weight composition 90:10. Only the PS block of the 30K component is deuterated.

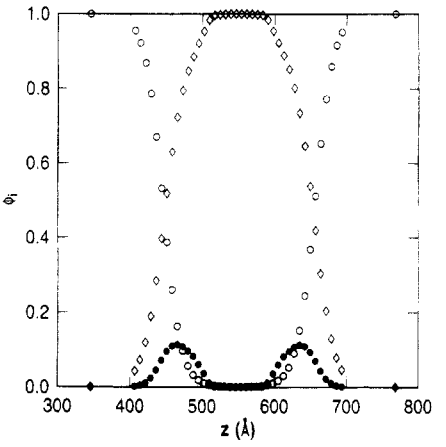

Figure 5. Volume fraction profiles of PS (○), d-PS (●), and PMMA (◇) within a characteristic domain of the 110K/30K mixture, deconvoluted from the *b*/*V* profile in Figure 6.

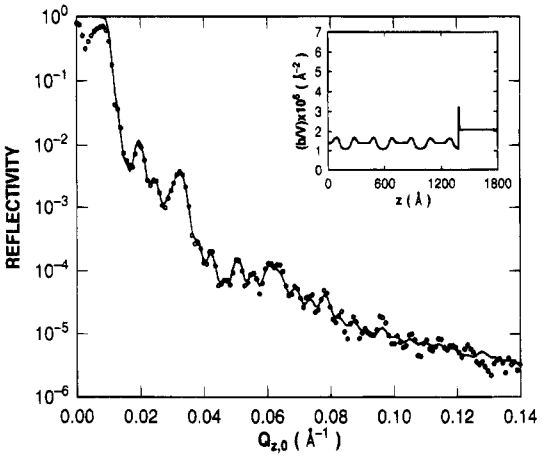

Figure 6. Fitted reflectivity data and model scattering length density profile (inset) for a 110K/30K mixture of weight composition 90:10. Only the PMMA block of the 30K component is deuterated.

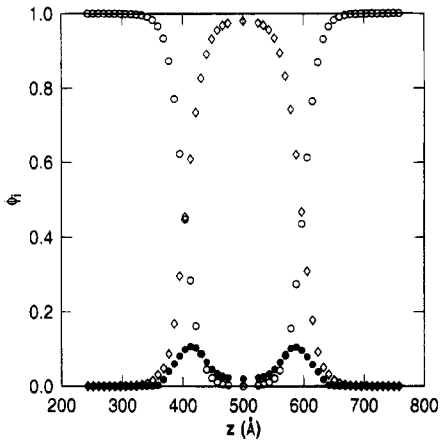

Figure 7. Volume fractions profiles of PS (○), PMMA (◇), and d-PMMA (●) within a characteristic domain of the 110K/30K mixture, deconvoluted from the *b/V* profile in Figure 8.

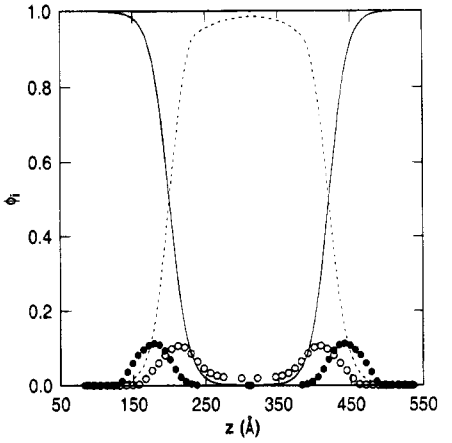

Figure 8. Distribution of PS (●) and PMMA (○) blocks of 30K material within the interface region, obtained by superposing two interfaces from Figures 5 and 7.

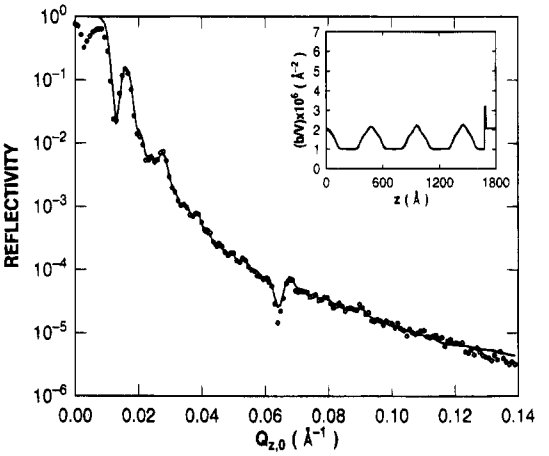

Figure 9. Fitted reflectivity data and model scattering length density profile (inset) for a 110K/300K mixture of weight composition 90:10. Only the PS block of the 300K component is deuterated.

length density profile are shown in Figure 6. It is interesting to compare these results to those in Figure 4. While the *b/V* profiles for the two labeling schemes exhibit similar features, the reflectivity profiles are significantly different, demonstrating the high degree of sensitivity afforded by this technique. Figure 7 shows the volume fraction profile for one characteristic domain of the mixture, evaluated from the scattering length density profile in the inset of Figure 6. The highest fraction of labeled PMMA (●) is again found in the interfacial regions between the PS (○) and PMMA (◇) microdomains, but the PMMA domain centers clearly contain a finite percentage of the 30K material. If one assumes that the domain centers contain extended blocks of labeled PMMA, then the integrated volume fraction of d-PMMA in the PMMA domains is 7.6%, compared to 9.3% calculated. The raised scattering length density in the PMMA domain centers could alternatively be explained by the dissolution of some portion of the 30K copolymer chains within the domains. A ~3% concentration of dissolved 30K chains would cause a comparable elevation of the *b/V* in the PMMA domain centers and would account for discrepancies in mass conservation for this mixture system.

The distribution of short chains within the lamellar domains is better seen by superposing two interfaces from Figures 5 and 7, as depicted in Figure 8. Although the 30K copolymer is highly localized to the interface, the PS and PMMA blocks of this material interpenetrate significantly. The solid and dashed lines in the figure represent respectively the concentration of PS and PMMA segments of the high molecular weight copolymer. The filled and open circles are respectively the PS and PMMA segments of the low molecular weight copolymer. The substantial degree of interpenetration translates to the expansion in interfacial width observed with the addition of the low molecular weight component. An alternative interpretation is that the lower molecular weight component increases the degree of fluctuation or waviness of the interface. In either case, for higher fractions of the 30K material the broadening is more pronounced, since a larger percentage of the interface is composed of short copolymer chains.

The component distributions were similarly examined in binary mixtures of the 110K and 300K copolymers. Figure 9 shows the reflectivity profile for a 90:10 mixture of the unlabeled 110K P(S-*b*-MMA) with a 300K P(d-S-*b*-MMA). Again, the solid line in the figure is the reflectivity profile calculated using the scattering length density profile in the inset. A comparison of the data in Figures 4 and 9 reveals that, though compositionally equivalent, the distribution of labeled material within these two systems is very different. The distribution of labeled and unlabeled blocks for the 110K/300K mixture is again seen to be nonuniform across the PS domains, as evidenced by the peaks in the scattering length density profile. Here, however, the labeled PS is concentrated to the domain centers. The volume

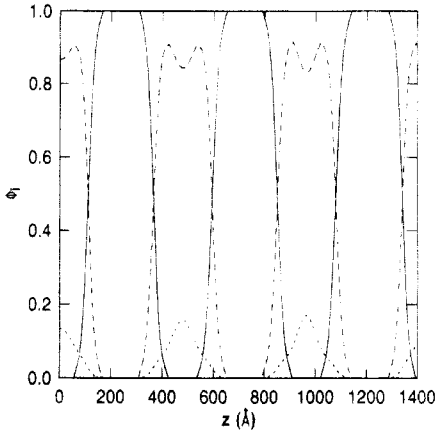

Figure 10. Volume fraction profiles of PS (– –), d-PS (• • •), and PMMA (—) from a 110K:300K mixture, deconvoluted from the *b/V* profile in Figure 11.

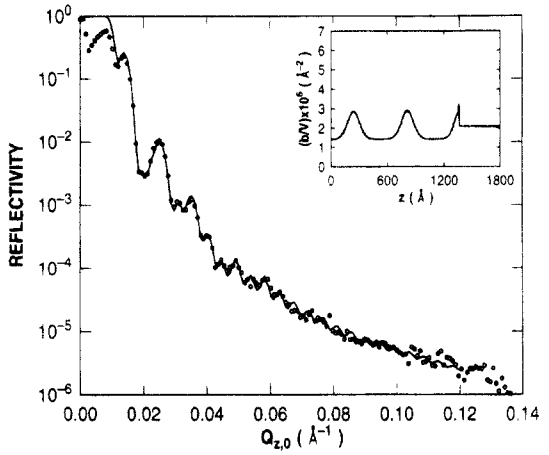

Figure 11. Fitted reflectivity data and model scattering length density profile (inset) for a 110K/300K mixture of weight composition 75:25. Only the PMMA block of the 300K component is deuterated.

fraction profiles for PS (– –), d-PS (• • •) and PMMA (—) across the entire film are shown in Figure 10. At the microdomain centers, the high molecular weight d-PS blocks are twice the average concentration. The block distributions appear to be quite consistent from layer to layer throughout the film, even within the surface half-layer. (A slightly lower fraction of 300K material may be indicated at the surface.) The integrated volume fraction of d-PS in the PS domains recovered from the model calculations is 9.5%, in excellent agreement with the volume fraction of 9.3% calculated for this mixture composition.

With higher concentrations of 300K material, the nonuniformity in the copolymer distribution is more pronounced. Figure 11 shows the reflectivity data for a 110K/300K 75:25 mixture where the PMMA block of the 300K copolymer is isotopically labeled. The scattering length density profile which gave the best fit to the data shows that the high molecular weight PMMA labeled blocks are concentrated in the domain centers. The volume fraction profile for the PS (—), PMMA (– –), and d-PMMA (• • •) derived from these results is plotted in Figure 12. The uniformity of the domain compositions throughout the film is again remarkable, with a slightly smaller fraction of 300K material present at the substrate. The integrated volume fraction of d-PMMA in the PMMA domains is 21.0%, in reasonable agreement with the calculated value of 23.6%.

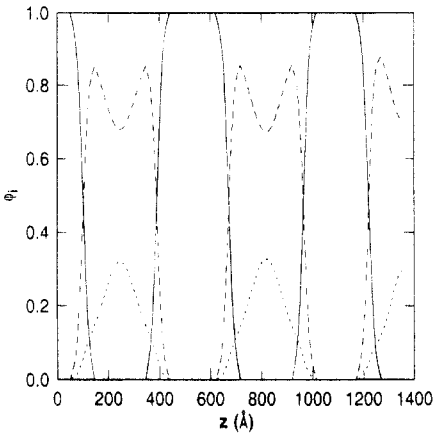

Figure 12. Volume fractions profiles of PS (—), PMMA (– –), and d-PMMA (• • •) from a 110K/300K mixture, deconvoluted from the *b/V* profile in Figure 13.

5. Conclusions

This work offers a quantitative demonstration of nonuniform distributions of components in ordered binary copolymer mixtures. Short-chain components are found to locate preferentially at the interface, while long chains concentrate in the domain centers. Such mixture schemes might be useful in preparing copolymer multilayers or other ordered structures which possess some localized functionality within the domains themselves.[4] The variation in the lamellar period for the mixtures is shown to be consistent with bulk results[19] in scaling with the number-average molecular weight to the $^2/_3$ power. The uniformity of the block distributions within the films suggests that, in strong segregation, film surfaces do not have long-range influences on the chain distributions. Thus, it is possible by reflectivity to garner what are effectively bulk details, not readily attainable with bulk characterization methods.

Noolandi and co-workers have recently employed self-consistent mean-field techniques to describe binary diblock copolymer mixtures in the ordered state.[33] Their model shows qualitative agreement with the results presented here, i.e., low molecular weight components are found in higher concentration near the interface regions. It also suggests partial solubility of low molecular weight copolymers within ordered domains for certain ranges of concentration, molecular weight, and molecular weight ratio of mixture components. Future work will compare more quantitatively the reflectivity results from copolymer mixtures with self-consistent-field calculations.

Acknowledgment. This material is based upon work supported in part by the Department of Energy. Office of Basic Energy Sciences, under Contract DE-FG03-88ER45375, and by the National Science Foundation under Grant No. DMR-9357602.

References and Notes

(1) Meier, D. J., Ed. *Block Copolymers: Science and Technology*; MMI Press/Harwood Academic Publishers: New York, 1983.
(2) Saunders, R. S.; Cohen, R. E.; Schrock, R. R. *Macromolecules* **1991**, *24*, 5599.
(3) Sankaran, V.; Cohen, R. E.; Cummins, C. C; Schrock, R. R. *Macromolecules* **1991**, *24*, 6644.
(4) Chan, Y.; Craig, G.; Schrock, R. R.; Cohen, R. E. *Chem. Mater.* **1992**, *4*. Yue, J.; Cohen, R. E.; Sankaran, V.; Schrock, R. R. *J. Am. Chem. Soc.* **1993**, *115*, 4409.
(5) Russell, T. P.; Karis, T. E.; Gallot, Y.; Mayes, A. M. *Nature* **1994**, *368*, 729.

(6) Helfand, E.; Wasserman, Z. R. *Macromolecules* **1976**, *9*, 879. Helfand, E.; Wasserman, Z. R. *Macromolecules* **1978**, *11*, 960. Helfand, E.; Wasserman, Z. R. *Macromolecules* **1980**, *13*, 994.
(7) Semenov, A. N. *Sov. Phys. JETP* **1985**, *61*, 733.
(8) Ohta, T.; Kawasaki, K. *Macromolecules* **1986**, *19*, 2621.
(9) Vavasour, J. D.; Whitmore, M. D. *Macromolecules* **1992**, *25*, 5477.
(10) Hasegawa, H.; Tanaka, H.; Yamasaki, K.; Hashimoto, T. *Macromolecules* **1987**, *20*, 1651.
(11) Hashimoto, T.; Shibayama, M.; Kawai, H. *Macromolecules* **1980**, *13*, 1237.
(12) Hashimoto, T.; Fujimura, M.; Kawai, H. *Macromolecules* **1980**, *13*, 1660.
(13) Hashimoto, T.; Tanaka, H.; Hasegawa, H. *Macromolecules* **1990**, *23*, 4378.
(14) Winey, K. I.; Thomas, E. L.; Fetters, L. J. *Macromolecules* **1991**, *24*, 6182.
(15) Winey, K. I.; Thomas, E. L.; Fetters, L. J. *Macromolecules* **1992**, *25*, 2645.
(16) Mayes, A. M.; Russell, T. P.; Satija, S. K.; Majkrzak, C. F. *Macromolecules* **1992**, *25*, 6523.
(17) Hadziioannou, G.; Shoulios, A. *Macromolecules* **1982**, *15*, 267.
(18) Hashimoto, T. *Macromolecules* **1982**, *15*, 1548.
(19) Hashimoto, T.; Yamasaki, K.; Koizumi, S.; Hasegawa, H. *Macromolecules* **1993**, *26*, 2895.
(20) Hashimoto, T.; Koizumi, S.; Hasegawa, H. *Macromolecules* **1994**, *27*, 1562.
(21) Almdal, K.; Rosedale, J. H.; Bates, F. S. *Macromolecules* **1990**, *23*, 4336.
(22) Leibler, L. *Macromolecules* **1980**, *13*, 1602.
(23) Coulon, G.; Ausserre, D.; Russell, T. P. *J. Phys. Fr.* **1990**, *51*, 777.
(24) Coulon, G.; Russell, T. P.; Deline, V. R.; Green, P. F. *Macromolecules* **1989**, *22*, 2581.
(25) Anastasiadis, S. H.; Russell, T. P.; Satija, S. K.; Majkrzak, C. F. *J. Chem. Phys.* **1990**, *92*, 5677.
(26) Mayes, A. M.; Russell, T. P. *J. Phys. IV. Colloq. C8* **1993**, *3*, 41.
(27) Mayes, A. M.; Johnson, R. D.; Russell, T. P.; Smith, S. D.; Satija, S. K.; Majkrzak, C. F. *Macromolecules* **1993**, *26*, 1047.
(28) Menelle, A.; Russell, T. P.; Anastasiadis, S. H.; Satija, S. K.; Majkrzak, C. F. *Phys. Rev. Lett.* **1992**, *68*, 67.
(29) Mezei, F. *Commun. Phys.* **1976**, *1*, 81.
(30) Hayter, J. B.; Mook, H. J. *Appl. Crystallogr.* **1989**, *22*, 35.
(31) Foster, M. D.; Sikka, M.; Singh, N.; Bates, F. S.; Satija, S. K.; Majkrzak, C. F. *J. Chem. Phys.* **1992**, *96*, 8605.
(32) Shull, K. R.; Mayes, A. M.; Russell, T. P. *Macromolecules* **1993**, *26*, 3929.
(33) Chi, A.-C.; Noolandi, J. *Macromolecules* **1994**, *27*, 2936.